Major Temporal Arcade Separation in Angiography Images of Retina Using the Hough Transform and Connected Components

Farshad Nabi[1] Hamed Yousefi[1] Hamid Soltanian-Zadeh,[1,2] *Senior Member, IEEE*

[1] CIPCE, School of Electrical and Computer Engineering, College of Engineering, University of Tehran, Tehran, Iran
[1,2] Image Analysis Laboratory, Radiology Department, Henry Ford Health System, Detroit, Michigan, USA

***Abstract*—Structural analysis of the vascular architecture of the retina is useful in facilitate the diagnosis of retinopathy disease. Retinopathy can affects the blood flow velocity. Measuring blood flow velocity in major temporal arcade (MTA) vessels in retina is one of the approaches to identify blood flow velocity changes. Hence separation of MTA vessel is a necessary step in blood flow velocity computation. We propose methods for separation of the MTA. We use Gabor filters to detect retinal vessels and Hough transform to model the MTA. Afterwards we use the MTA model to find initial point of MTA. Next we take advantage of connected components to track temporal arcade vessel, and separate the MTA. Results obtained with applying our algorithm to 24 clinical angiography images, in which traces of MTA was drawn with an ophthalmologist expert, indicating 92% correct separation of MTA.**

Keywords—Blood vessels; angiography images; Gabor filters; Hough transform; retinopathy; major temporal arcade.

I. Introduction

A. Diabetic Retinopathy

Diabetic Retinopathy (DR) is one of the most epidemic diseases of human visual system which is caused by the increase of glucose level in blood vessels. In addition, this disease is responsible for early blindness of patients younger than 70 years in developed countries [1]. Statistics indicate that the risk of blindness in diabetic patient is 25 times more than healthy subjects [2]. In the past, it was believed that structural changes such as Hemorrhages and presence of red lesions in the eye are the first symptoms of DR and as a result the disease was not detected until the occurrence of visual loss and total impairment of the visual acuity. Most of the methods for prevention and treatment of diabetic retinopathy are based on retinal morphological variations such as microaneurysms and exudates [3], [4], [5]. Nevertheless recent procedure had spotted DR by looking at the functional variations which happen before structural variations. One of this functional information is blood flow velocity variations which occur before any other morphological changes [6].

The blood flow velocity is higher in patients with early diabetes mellitus than healthy subjects. This process is caused due to increment of blood glucose for a long duration that impresses structure and function of blood vessels wall. Recently, Zvia Burgansky-Eliash et al used Retinal Functional Imager (RFI) to determine retinal blood flow velocity [6].

The RFI (designed in Optical Imaging Ltd Co, Rehovot, Israel) [7], [8] is an ophthalmic imaging device which depicts retina to a high resolution image and as a result, tiny red blood cells moving through vessels become observable. These tiny red blood cells could not be observed by other ophthalmic imaging apparatus before. RFI calculates blood flow velocity by tracking retinal red blood cells in a short movie (8-24 frames) taken under green light.

B. Major Temporal Arcade (MTA) Separation and Modeling

The detection of temporal arcade can help in blood flow velocity computation and localization of optic nerve head and fovea [9]. Major temporal arcade can be segmented using Hough transform [9] on the segmented vessels.

Niemeijer et al. [10] used a point distribution model to represent the major temporal arcade using a set of 10 points to mark the MTA. They used five hundred images to minimize a cost function and obtain a set of parameters. The cost function was consisted of two global terms, width and orientation of vessels, and one local term, anatomic measurements around model points. The optimization was applied in both image and parameter space. When parameters were obtained, they are used in an image using the same optimization to obtain a point distribution model. A human observer checks how many of ten points lies correctly on the MTA. Niemeijer et al. reported 93.2% complete detection of the MTA, 5.6% partial detection, and 1.2% complete failure to detect the MTA in 500 images of the retina.

Fleming et al. [11] used vessel enhancement and semielliptical curve fitting using the generalized Hough transform to model the MTA. After enhancing the vessels and obtaining an edge map of the vessels, the generalized Hough Transform was applied to skeletonized image of the vasculature. The Global maxima in Hough space was chosen as the best match for MTA model.

The previously published methods to model the MTA, as explained in section I-B, do not practically extract the MTA vessel. Furthermore coordinate of the center of optic disc is considered as the vertex of temporal arcade angle. Extraction and separation of MTA is essential in blood flow velocity computation, which is one of the strongest features in diagnosis of the retinopathy disease. In this paper we propose a method to extract and separate the MTA using Gabor filters, Generalized Hough transform and connected components.

II. METHODS

A. Preprocessing

The proposed methods were tested with angiography images of the retina from the Feiz hospital in Isfahan-Iran. These images were taken by Heidelberg Retina Angiograph 2 (HRA2) which is a confocal laser scanning system for digital fluorescent and indocyanine green angiography. The laser origin includes in the HRA2 diffuse laser light for fluorescent angiography with 488 nm wavelength. To perform angiography test, Fluorescein is injected into an arm's vein and fundus camera is used to image the retina. The most important application of fluorescent angiography imaging is to detect microaneurysm in retina by morphological operators [12], [13]. Another advantage of fluorescent angiography imaging compared to other retinal imaging methods is that red lesions are more easily identified as a result of high contrast with the background [14], [15], [16]. Recently, video capture device was added to the HAR2 apparatus. angiographic videos for calculating the blood flow velocity in arteries which are not utilized for this purpose; while Zvia Burgansky-Eliash et al used RFI which represent an approach for calculating the blood flow velocity in vessels, mapping vessels structure, and acquiring oximetric and metabolic status of retina.

The first two-steps algorithms increase the contrast of retina between vessel and non-vessel pixels. Since typical enhancement methods are not appropriate for extracting the vessels from retina in the angiography images [17], [18], we took advantages from the Gabor transform followed by Laplacian-of-Gaussian (LoG) filter [19]. Next retinal blood vessels were extracted using statistical local threshold (SLT).

The Laplacian is the 2D isotropic derivative of image which is used to find regions with fast intensity changes (edge detection). Since the 2D derivative is very sensitive to noise, we reduced the noise by using a Gaussian filter. Applying these two operators to an image is named LoG which is:

$$L_{\sigma}(p;\sigma)=(\nabla^{2}M(n;\sigma))*I(n) \tag{1}$$

Where ∇^2 is the Laplacian operator, M(n;σ) is an isotropic zero mean Gaussian kernel and σ^2 is the kernel's variance. "*"stands for the convolution operation and I is the grayscale format of the input image. Finally, the image was convolved with the LoG filter and the output was thresholded to obtain the largest values in the image:

$$L(p)=\max_{\sigma} L_{\sigma}(p;\sigma) \tag{2}$$

In order to improve image contrast, we applied a Gabor wavelet filter to the image. The Gabor wavelet filter is a sinusoidal component multiplied by the Gaussian kernel[18] as followed,

$$B(p;\lambda,\alpha,\theta)=s(p;\lambda)\ M(p;\alpha,\theta) \tag{3}$$

Where s (.) is the sinusoidal component and *M (·)* is an anisotropic, scaled, and rotated Gaussian function. We applied the filter with different wavelength *(λ)*, scale *(α)* and orientation *(θ)*. The maximum respond is obtained by varying *(λ), (α) and (θ)* and is defined by[16]:

$$G(p)=\max_{\lambda,\alpha,\theta}(L(p)*B(p;\lambda,\alpha,\theta)) \tag{4}$$

Fig. 1. shows the results of image enhancement step.

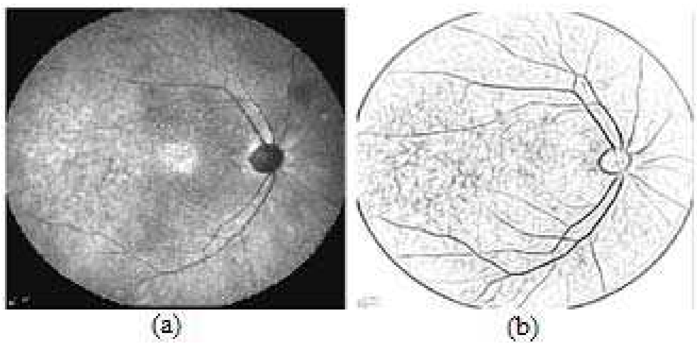

Fig.1. (a) angiography image, (b) Output of Gabor filter following LOG

Some errors occur in vessel extraction step owing to the fact that the quality of background is not uniform throughout the whole for the entire retina. However, SLT provides improvement by dividing the image into non-overlapping rectangles based on their non-uniformly distributed intensity. Afterwards, they should be divided into uniformly distributed intensity rectangles.
SLT is defined as:

$$T_{xy}=a.m_{xy} \tag{5}$$

An 11×11 window was considered for each pixel and the mean intensity was calculated as followed,

$$m_{xy}=\frac{1}{11^2}\sum_{x-5}^{x+5}\sum_{y-5}^{y+5}I(x,y) \tag{6}$$

In which m_{xy} is the mean intensity in the selected window, $I(x,y)$ is the image intensity and a is a constant coefficient for changing the accuracy of vessel extraction, noise variations and vessels accretion.
After calculation of SLT, the image is segmented by using the following thresholds:

$$g(x,y)=\begin{cases}0 & I(x,y)>T_{xy}\\ 1 & I(x,y)\le T_{xy}\end{cases} \tag{7}$$

In (7), 0 is defined for background and 1 is considered for the vessels .In this calculation, the coefficient α changes the classification sensitivity. The possibility of choosing the microaneurysm as a vessel gets higher after increasing α content. Fig. 2. Shows the result of applying SLT on an angiography image.

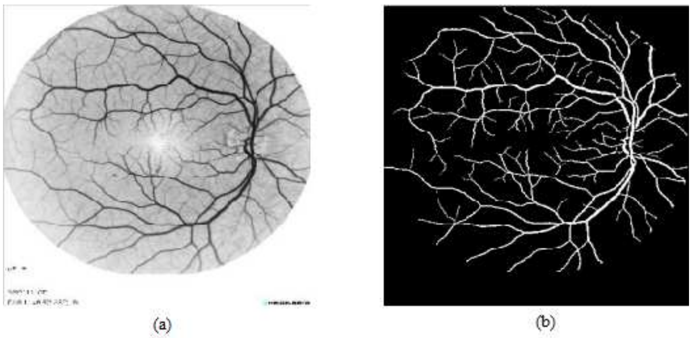

Fig.2. (a) angiography image, (b) Output of SLT algorithm.

B. Hough Transform

Hough [20] proposed an approach to find lines in an image. We can generalize the Hough transform to detect other parameterized curves like parabolas [21], [22], [23], [24]. Here we define a parabola with its directrix parallel to the y-axis and its symmetrical axis parallel to the x-axis as follows:

$$(y - y_0)^2 = 4a(x - x_0)^2 \tag{8}$$

Where $(x - x_0)$ is the vertex of the parabola and the quantity $4a$ is known as the latus rectum. The value of a defines the aperture of the parabola and indicates the direction of the opening of the parabola; for a positive value, the parabola opens to the right. The parameters (x_0, y_0, a) define the Hough space. Every non-zero pixel in the image is corresponded to a parabola in Hough space for each value of a . Each point in the Hough space defines a parabola in the image domain. The size of (x_0, y_0) planes in the Hough space is the same as the size of images (768 × 868 pixels). The value of a is restricted by physiological limits on the arcade and the size of the image. For our database, the value of a was translated to the range [30, 60]. We consider only positive values of a were defined. For images with the temporal arcade opening to the left, it was rotated by 180◦ so the arcade would open to the right.

We applied the Hough transform to the vessel map images. The point with highest value in the Hough space was used to model the parabola for MTA. This model is used to track and separate the MTA vessel.

C. Connected Components and MTA tracking

In graph theory, a connected component (or just component) of an undirected graph is a sub-graph in which any two vertices are connected to each other by paths, and which is connected to no additional vertices in the super graph. Connected component labeling works by scanning an image, pixel-by-pixel (from top to bottom and left to right) in order to identify connected pixel regions, *i.e.*regions of adjacent pixels which share the same set of intensity values *V*. (For a binary image V={1}). We use connectivity feature to track MTA vessel. After some pruning procedures on the obtained vessel map, we create a profile of connected component in each angle. Connected components are investigated in an interval around the current angle θ. Fig. 3. Shows the way, connected components profile at the angle θ is created.

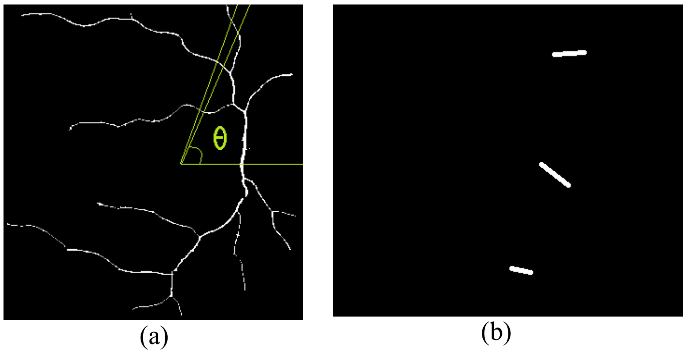

Fig. 3. (a) A pruned vessel map image. (b) Connected component profile of image (a) at the angle θ .

As we see in fig. 3. (a) there is three connected components in the interval [θ, $\theta + \Delta\theta$]. In this work we used $\Delta\theta = 10$. Now if we know which connected component is related to MTA, then we can keep that and throw away the others. For this purpose we used the MTA model. As the parabola model is more correlative with the MTA near the optic disc, we used the angle $\theta_0 = 30$ to choose the initial connected component related to MTA vessel. We used $\theta_0 = 30$ because it was the optimum angle as it is neither so close to the optic disc ($\theta = 0$), where is the origin of all vessels, nor so far, where the MTA vessel and parabola model diverges. Fig. 4. Shows how we choose the initial connected component using the MTA model.

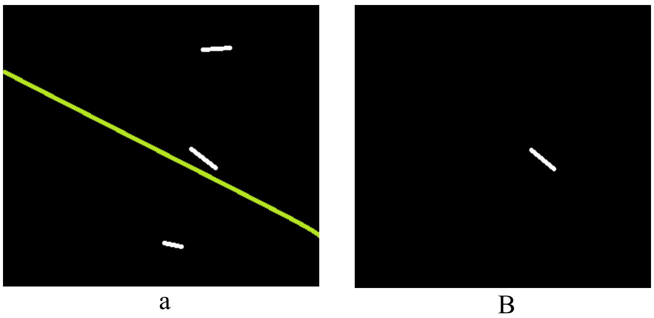

Fig. 4. (a) MTA model drawn with green line and connected component profile at angle $\theta = 30$. (b) Connected component which is closer to the MTA model.

We compute center of gravity of each component and then calculate the distance between them and the MTA model to find the closest one. This closest component is called initial component and it can initiate the MTA tracking procedure. Next step is investigating connected components at angle

$\theta = \theta_0 + \Delta\theta$. In a general form we can rewrite this equation as follows:

$$\theta_{i+1} = \theta_i + \Delta\theta \quad (9)$$

Note: if we are moving counter clockwise, $\Delta\theta = +10$,otherwise $\Delta\theta = -10$.

At the next step we are going to fine the closest connected component to the initial component of previews step. Considering the closest component of each step as new initial component, we can track the vessel related to the first initial component. In each angle only one component is preserved and other components are thrown away. This means only MTA is tracked and other vessels and their branches are removed. It can explained for an overview that we start from θ_0 and then continue toward the bottom and origin of the MTA vessel. We should move counter clockwise to reach the bottom of the MTA vessel, and investigate θs greater than θ_0 , which are set of θs that we name θ_f :

$$\theta_f = \{\theta_0 + \Delta\theta, \theta_0 + 2\Delta\theta, ..., 180\} \quad (10)$$

To reach the origin of MTA vessel we need to move clockwise, and investigate θs smaller than θ_0, which are set of θs that we name θ_b :

$$\theta_b = \{\theta_0 - \Delta\theta, \theta_0 - 2\Delta\theta, ..., 0\} \quad (11)$$

These are procedures to find the upper section of the MTA, and to find lower section of it we should do the procedures for $\theta_0 = -30$, and except for θ_0 all the steps are the same.

The whole algorithm is summarized in fig. 5.

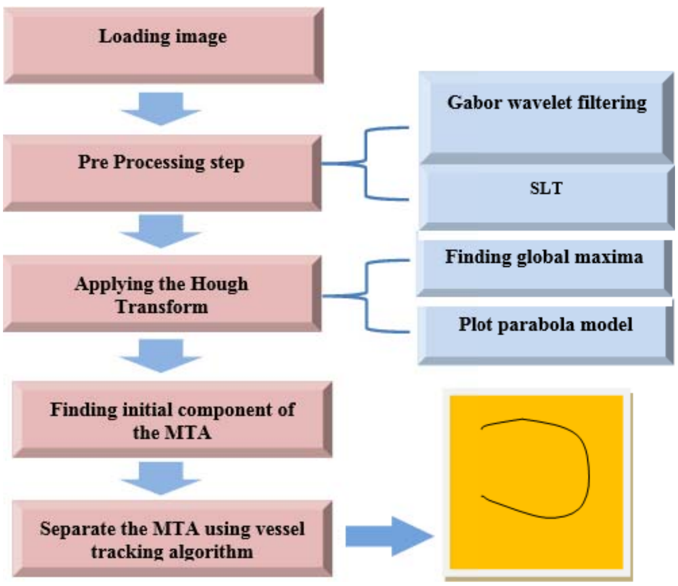

Fig. 5. Block diagram of the proposed method.

III. EXPERIMENTAL RESULTS

Fig. 6. (a) shows one of the original images of our database. Fig. 6. (b) shows the result of applying Log and Gabor wavelet filtering to improve the contrast of image. Fig. 6. (c) shows the result of applying SLT, in order to create a binary image and segment vessels. Fig. 6. (d) after applying generalized Hough transform to vessel map image, the parabola with the highest value was obtained for $\alpha = 56$; this parabola model is drawn on the vessel map image with green color. Fig. 6. (e) shows the MTA vessel, which is separated using initial component obtained from parabola model, and vessel tracking algorithm.

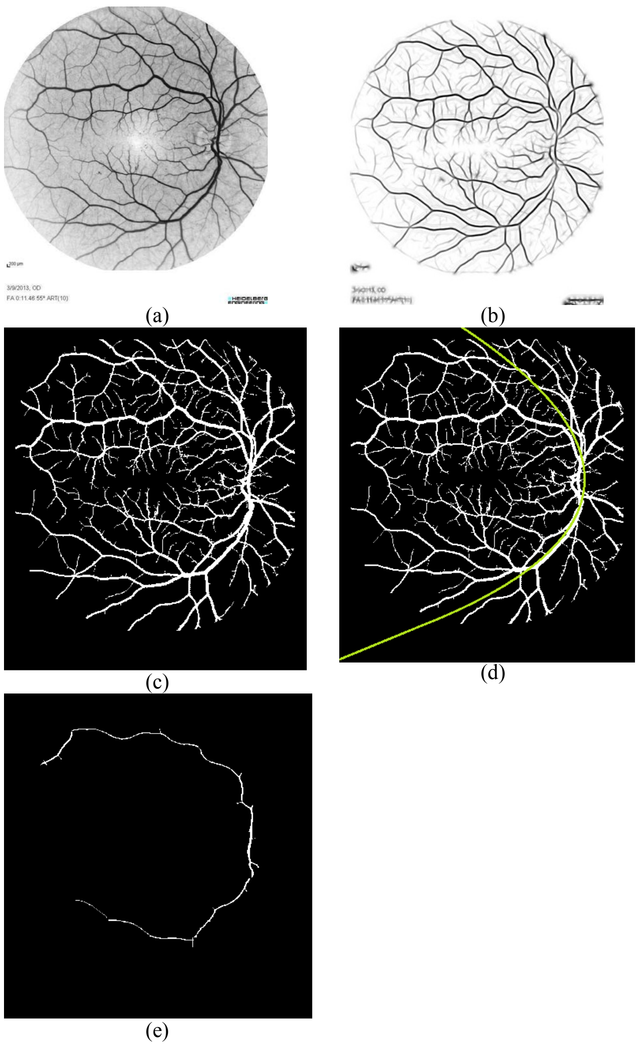

Fig. 6. (a) One of the original images of our database. (b) Original image after preprocessing including LoG and Gabor wavelet filtering. (c) extracted vessel using SLT. (d) Extracted vessels with the parabola model of MTA which is drawn with green line. (e) Extracted MTA using proposed algorithm.

The result of MTA separation using the Hough transform and connected components applied to 24 angiography images of Feiz hospital database, indicated 22 correct separation, and 2 wrong separation. If the separated vessel was MTA, we would consider it as correct separation, and if it was other vessel, we would consider it as wrong separation. MTA vessels were drawn by an ophthalmology expert.

We compared the hand drawn MTAs with extracted MTAs using XOR operator:

$$T = H \otimes E \tag{12}$$

Where H is the binary hand drawn image of MTA, and E is the extracted MTA image. Next we calculated the portion of number of ones in T to number of image pixel:

$$P = \frac{\sum_{Pixels} T}{N} \tag{13}$$

Where N is number of pixels in the image. Then depending on the value of P, we decided to consider the extracted MTA as correct or as incorrect separation:

$$\begin{cases} P \leq 0.01 & \textit{correct separation} \\ P > 0.01 & \textit{incorrect separation} \end{cases} \tag{14}$$

IV. DISCUSSION AND CONCLUSION

Using SLT approach for thresholding of Gabor wavelet response is more sensitive to find minor vessels than fixed thresholding. We can use fixed thresholding to prevent the detection of minor vessels. Pruned vessel map have better fitted parabola, and consequently it is more likely to result a correct MTA extraction. Beside acceptable results of this work there is some limitations, need to be addressed. In some cases the opening of the MTA is not precisely toward right or left, and it has a little tendency to the top or bottom; it is not considered in modeling the MTA. Finding the correct initial component at the beginning is very dependent on the amount of fitness of parabola model to MTA. If we could use a cost function to consider other features like thickness of connected components, then we could have more accurate and robust MTA detection algorithm.

In previous works they just calculate a model for MTA, and do not practically extract the MTA vessel. MTA model is beneficial, but in some applications like blood flow velocity computation we need to have the MTA vessel. In [10], Niemeijer et al. introduce a point distribution model, which fits to the vascular arc of image. In [9], Oloumi et al. use the Hough transform to model the MTA but they don't go further to extract the MTA vessel itself. In [11], Fleming et al. used vessel enhancement and semielliptical curve fitting using the generalized Hough transform to model the MTA. In this work, we took advantage of connected components to extract the MTA vessel in addition to defining a model using the Hough transform.

The proposed method had a good result in separation of the MTA vessel of angiography images. Extracted MTA can be used in blood flow velocity calculation of angiography videos; so it is beneficial for diagnosis and therapy of retinopathy.

ACKNOWLEDGMENT

A lot of thanks to Dr. Mohammadreza Akhlaqi for guiding us, and Feiz hospital in Isfahan-Iran, for providing us angiography images of retina.

REFERENCES

[1] R. Klein, B. E. Klein, "Vision disorders in diabetes", Diabetes in America, vol. 1, pp. 293-338, (1995).

[2] Centers for disease control and prevention (CDC)., "Public health focus: preventation of blindness associated with diabetic retinopathy", MMWR Morb Mortal Wkly Rep, 19;42(10):191-195, 1993.

[3] S. N. Shajahan, R. C. Roy, "An Improved Retinal Blood Vessel Segmentation Algorithm based on Multi-structure Elements Morphology", I. J. Computer Applications, vol. 57, pp. 8875 – 8887, 2012.

[4] M. Kalaivani, M. S. Jeyalakshmi, V. Aparna, "Extraction Of Retinal Blood Vessels Using Curvelet Transform And Kirsch's Templates", I. J. Emerging Technology and Advanced Engineering, vol. 2, pp. 2450-2459, 2012.

[5] L. Zhou, M. S. Rzeszotarski, L. J. Singerman, and J. M. Chokreff, "The detection and quantification of retinopathy using digital angiograms", IEEE Trans. Med. Imag., vol. 13, pp. 619–626, 1994.

[6] Z. Burgansky-Eliash, A. Barak, H. Barash, D. A. Nelson, O. Pupko, A. Lowenstein, A. Grinvald, and A. Rubinstein, "Increased retinal blood flow velocity in patients with early diabetes mellitus, Retina", vol. 32, pp. 112-119, 2012.

[7] M. D. Abràmoff, Y. H. Kwon, D. Ts'o, P. Soliz, B. Zimmerman, J. Pokorny, and R. Kardon, "Visual stimulus–induced changes in human near-infrared fundus reflectance", Investigative ophthalmology & visual science, vol. 47, pp. 715-721, 2006.

[8] A. Grinvald, T. Bonhoeffer, I. Vanzetta, A. Pollack, E. Aloni, R. Ofri, and D. Nelson, "High-resolution functional optical imaging: from the neocortex to the eye", Ophthalmology clinics of North America, pp. 53-68, 2004.

[9] F. Oloumi, and R.M.Rangayyan, " Detection of the Temporal Arcade in Fundus Images of the Retina Using the Hough Transform", International Conference of the IEEE EMBS, vol. , pp. 3585-3588, september. 2009.

[10] M. Niemeijer, M. D. Abràmoff, and B. van Ginneken, "Segmentation of the optic disk, macula and vascular arch in fundus photographs," IEEE Trans. Med. Imag., vol. 26, no. 1, pp. 116–127, Jan. 2007.

[11] A. D. Fleming, K. A. Goatman, S. Philip, J. A. Olson, and P. F. Sharp, "Automatic detection of retinal anatomy to assist diabetic retinopathy screening," Phys. Med. Biol., vol. 52, no. 2, pp. 331–345, Jan. 2007.

[12] C. E. Baudoin, B. J. Lay, and J. C. Klein, "Automatic detection ofmicroaneurysms in diabetic fluorescein angiography", Rev. Epidemiol.Sante Publique, vol. 32, pp. 254–261, 1984.

[13] M. Sonka, V. Hlavac, and R. Boyle, Image Processing, Analysis, and Machine Vision, 3rd ed. Toronto, Canada: Thomson Engineering, 2008.

[14] T. Spencer, J. A. Olson, K. C. McHardy, P. F. Sharp, and J. V. Forrester, "An image-processing strategy for the segmentation and quantification of microaneurysms in fluorescein angiograms of the ocular fundus," Comput. Biomed. Res., vol. 29, pp. 284–302, 1996.

[15] A. J. Frame, P. E. Undrill, M. J. Cree, J. C. Olson, K. C. Mchardy, P. F. Sharp, and J. V. Forrester, "A comparison of computer based classification methods applied to the detection of microaneurysms in ophthalmic fluorescein angiograms", Comput. Biol. Med., vol. 28, pp. 225–238, 1998.

[16] M. J. Cree, J. A. Olson, K. C. McHardy, P. F. Sharp, and J. V. Forrester, "A fully automated comparative microaneurysm digital detection system", Eye, vol. 11, pp. 622–628, 1997.

[17] J. L. Starck, F. Murtagh, E. J. Candes, and D. L. Donoho, "Gray and color image contrast enhancement by the curvelet transform", Image Processing, IEEE Trans, vol. 12, pp. 706-717, 2003.

[18] T. Acharya and A. Ray, Image Processing: Principles and Applications, Wiley-Interscience, 2005.

[19] R. Estrada, C. Tomasi, M. T. Cabrera, D. K. Wallace, S. F. Freedman, and S. Farsiu, "Exploratory Dijkstra forest based automatic vessel segmentation: applications in video indirect ophthalmoscopy (VIO)", Biomed optics express, vol. 3, pp. 327-338, 2012.

[20] Hough PVC, "Method and means for recognizing complex patterns," US Patent 3, 069, 654, December 18, 1962.

[21] Rangayyan RM, Biomedical Image Analysis, CRC, Boca Raton, FL, 2005.

[22] Jafri MZM and Deravi F, "Efficient algorithm for the detection of parabolic curves," Vision Geometry III, vol. 2356, pp. 53–62, 1994.

[23] Ballard DH, "Generalizing the Hough transform to detect arbitrary shapes," Pattern Recognition, vol. 13, no. 2, pp. 111–122, 1981.

[24] Wechsler H and Sklansky J, "Finding the rib cage in chest radiographs," Pattern Recognition, vol. 9, no. 1, pp. 21–30, 1977.